



Title	Microbial abundance and community composition in biofilms on in-pipe sensors in a drinking water distribution system
Author(s)	Kitajima, Masaaki; Cruz, Mercedes C.; Williams, Rohan B. H.; Wuertz, Stefan; Whittle, Andrew J.
Citation	Science of the total environment, 766, 142314 https://doi.org/10.1016/j.scitotenv.2020.142314
Issue Date	2021-04-20
Doc URL	http://hdl.handle.net/2115/86709
Rights	© <2021>. This manuscript version is made available under the CC-BY-NC-ND 4.0 license https://creativecommons.org/licenses/by-nc-nd/4.0/
Rights(URL)	https://creativecommons.org/licenses/by-nc-nd/4.0/
Type	article (author version)
File Information	Clean_STOTEN_Manuscript_Revision2_v.pdf



[Instructions for use](#)

ABSTRACT

1
2 Collecting biofilm samples from drinking water distribution systems (DWDSs) is challenging
3 due to limited access to the pipes during regular operations. We report here the analysis of
4 microbial communities in biofilm and water samples collected from sensors installed in a DWDS
5 where monochloramine is used as a residual disinfectant. A total of 52 biofilm samples and 14
6 bulk water samples were collected from 17 pipe sections representing different water ages.
7 Prokaryotic genome copies (bacterial and archaeal 16S rRNA genes, *Mycobacterium* spp.,
8 ammonia-oxidizing bacteria (AOB), and cyanobacteria) were quantified with droplet digital PCR,
9 which revealed the abundance of these genes in both biofilm and water samples. Prokaryotic 16S
10 rRNA gene sequencing analysis was carried out for a subset of the samples (12 samples from four
11 sites). *Mycobacterium* and AOB species were dominant in the DWDS sections with low water
12 age and sufficient residual monochloramine, whereas *Nitrospira* species (nitrite-oxidizing
13 bacteria) dominated in the sections with higher water age and depleted monochloramine level,
14 suggesting the occurrence of nitrification in the studied DWDS. The present study provides novel
15 information on the abundance and identity of prokaryotes in biofilms and water in a full-scale
16 operational DWDS.

17
18 **Key words:** Water distribution system; biofilm; water quality; 16S rRNA gene sequencing;
19 nitrification

20 **1. Introduction**

21 Drinking water distribution systems (DWDSs) are an essential urban infrastructure that must
22 be adequately managed in order to provide safe and high-quality drinking water to end-point
23 consumers. However, water quality may deteriorate during distribution due to microbial
24 processes in DWDS, including biofilm development (Liu et al., 2013). Biofilms occur universally
25 in DWDS and are usually considered undesirable, because they are known to be the primary
26 cause of many issues in drinking water quality, including nitrification, residual disinfectant decay,
27 proliferation of pathogens, and aesthetic problems in color, odor, and taste (Liu et al., 2016;
28 Zhang et al., 2009). Biofilms comprise communities of microorganisms that attach to surfaces
29 through extra-cellular polymeric substances. Numerous factors can influence biofilm formation
30 and growth in DWDS, including water characteristics (such as microbial numbers, nutrient
31 concentration, temperature), pipe material, hydraulic conditions, and levels of residual
32 disinfectant (which decays with water age) (Wang et al., 2012).

33 Many water utilities have switched from chlorine to chloramines for secondary disinfection
34 of drinking water, primarily to reduce the formation of disinfection byproducts (Seidel et al.,
35 2005). Chloramines also maintain disinfection residuals for a longer period throughout the
36 distribution system (Norton and LeChevallier, 1997) and may penetrate biofilms more effectively
37 (Lee et al., 2011). However, one major drawback of chloramination is nitrification where
38 ammonia is sequentially oxidized to nitrite and nitrate. Ammonia-oxidizing bacteria (AOB)
39 and/or archaea (AOA) oxidize ammonia to nitrite, while nitrite-oxidizing bacteria (NOB) convert
40 nitrite to nitrate (Zhang et al., 2009). Residual ammonia can be present in chloraminated water
41 from the reaction between chlorine and ammonia intended to produce monochloramine.
42 Additional ammonia can be formed as a result of oxidization of the intermediate nitrite by
43 chloramines, which in turn accelerates nitrification and residual chloramine decay (Zhang et al.,
44 2009). Production of toxic nitrite and nitrate as well as the growth of heterotrophic bacteria,

45 (which may include opportunistic waterborne pathogens associated with loss of disinfectant) pose
46 risks to public health.

47 Nitrifiers (i.e., AOB, AOA, and NOB) are known to dwell in biofilms that provide them with
48 protection against disinfectants. Understanding the role and ecology of biofilms in DWDS is
49 therefore essential to develop effective strategies for management of water quality problems
50 including nitrification. The collection of biofilm samples from pipe walls within operational
51 DWDS presents a substantial challenge due to limitations in accessing the underground pipe
52 distribution network. Prior studies have used model systems (bench-top or pilot scale systems in
53 the laboratory) or have speculated on the development of biofilms based on tap water samples
54 and associated environmental factors (Abbaszadegan et al., 2015; Gomez-Alvarez et al., 2014;
55 Lee et al., 2011; Schwake et al., 2015; Wang et al., 2012). Although these studies have
56 contributed significantly to our understanding of biofilm growth within DWDS, model systems
57 inevitably differ from actual DWDS in terms of key hydraulic and environmental variable
58 including pressure, flow rate, water age, and local water quality. In addition, there are critical
59 limitations of using tap water samples containing only planktonic cells to infer biofilm
60 community, because of the distinction between planktonic and biofilm communities in DWDS
61 (Douterelo et al., 2013). To overcome these limitations, some efforts have been made to study
62 biofilms *in situ* in full-scale operational DWDS by collecting samples from a device inserted into
63 the pipe (Douterelo et al., 2014), water meters (Hong et al., 2010; Koskinen et al., 2000; Ling et
64 al., 2016; Lührig et al., 2015; Watson et al., 2004), or pipe samples (Cruz et al., 2020; Kelly et al.,
65 2014; Liu et al., 2020; Lührig et al., 2015)(Douterelo et al., 2020). Some previous studies also
66 employed full-scale experimental DWDS that accurately replicates the hydraulic and other
67 physical, chemical, and biological conditions of operational DWDSs (Douterelo et al., 2013; Fish
68 et al., 2015). However, relatively little is known about the spatial distribution of microbial species
69 and ecology across a full-scale operational DWDS.

70 The purpose of the present study was to investigate microbial abundance and composition in
71 a full-scale operational chloraminated DWDS by analyzing microbial communities colonizing
72 WaterWiSe sensors within a large DWDS. WaterWiSe is a wireless sensor network consisting of
73 in-pipe, online sensors (Allen et al., 2011), and was deployed to monitor the integrity of DWDS
74 by measuring hydraulic and basic water quality parameters including pressure/acoustics, flow
75 rate, pH, oxidation-reduction potential (ORP), conductivity, and fluorescent dissolved organic
76 matter. This system also provides a unique opportunity to study the microbiology within an
77 operational DWDS. The insertion probe for each sensor node provides a variety of substrate
78 materials (i.e., brass, stainless steel [SS], polyvinyl chloride [PVC], polyoxymethylene [POM])
79 for accumulation of biofilms and also allows collection of flowing bulk water from a local
80 sampling port (on the probe). Here, we report the analysis of microbial population and
81 composition in both biofilm and water phase samples to understand microbial ecology and
82 associated processes that may impact local water quality in a chloraminated DWDS.

83

84 **2. Materials and Methods**

85 *2.1. Sampling design*

86 A sampling campaign was designed to collect bulk water and biofilm samples from the
87 hydraulic and water quality sensors installed in a testbed network covering a 60-km² area. The
88 water source in this area is a blend of treated surface water and desalinated seawater, which is
89 supplied by a gravity-fed DWDS consisting of two service reservoirs. Monochloramine has been
90 used as a residual disinfectant in the system since 2005.

91 In February 2014, WaterWiSe sensors that had been operating at 17 sites (sampling site ID:
92 S1 to S17; actual locations of these sensors are indicated in Figure S1 in the Supplementary
93 Material) across the DWDS were replaced for periodic maintenance. The original sites were
94 chosen to optimize detection of hydraulic (bursts and leaks) and contamination events within the

95 pipe network. In-pipe water quality sensors were inserted in the center of the water pipe, and had
96 been in service for periods ranging from 6 to 18 months at the time of sampling (biofilm age,
97 Table 2). The studied DWDS can be sub-divided into two zones characterized by different water
98 ages (retention time from the service reservoirs), with lower water ages in Zone 1 (3.1 to 20.1 h)
99 compared to Zone 2 (35.9 to 45.1 h) based on EPANET simulations (Rossman, 2000), Table 1.
100 Because Zone 1 covers a larger geographical area than Zone 2 (Figure S1), the testbed included
101 higher number of sensor locations (sampling sites) in Zone 1 (15 sites) as compared to Zone 2 (2
102 sites). There were two versions of sensors that had been installed in the test bed: *A*) with a
103 sampling tap on the top of the sensor unit that allowed collection of water sample from the
104 middle of the water pipe through a tube in the insertion rod mechanism, and allowed collection of
105 biofilm samples on four different types of sensor substrata, i.e., brass, SS, PVC, and POM
106 (DuPont™ Delrin®) with sampled surface area of 77.4, 6.5-19.6, 113.0, and 28.3-53.4 cm²,
107 respectively; and *B*) without the bulk water sampling tap, and two different types of sensor
108 surface material (i.e., SS and POM with sampled surface area of 185.3 and 78.5 cm²,
109 respectively) were available for biofilm sample collection (see Figure S2 for the photographs of
110 these sensors). The version B sensors had been installed at two sites (i.e., S2 and S4), while the
111 version A sensors had been installed at the remaining 15 sites.

112 *2.2. Collection of bulk water and biofilm samples*

113 A total of 52 biofilm samples (up to four samples from different types of sensor surface per
114 site [brass, SS, PVC, POM]) and 14 bulk water samples were collected from 17 sensor
115 installation sites. One biofilm sample (n = 1) was collected from each surface type of each sensor,
116 and up to 5 L of bulk water was collected concomitantly from each site. Some samples were not
117 available due to technical difficulties in sampling, which resulted in fewer samples than the
118 expected maximum numbers (i.e., a total of 64 biofilm and 15 bulk water samples).

119 At each sampling site, bulk water samples were collected from the sampling tap (where

120 available) after flushing water from the tap for >5 mins, which was done before sensor
121 replacement. Physicochemical parameters, such as temperature, conductivity, total dissolved
122 solids (TDS), and salinity, were measured in the field immediately after sample collection using a
123 portable HI 9828 Multiparameter meter (Hanna Instruments, Inc., Woonsocket, RI). Free and
124 total chlorine were measured with a DPD colorimetric method using the Lovibond® Comparator
125 2000+ and tablet reagents (Tintometer Ltd., Amesbury, UK). Turbidity was measured using a
126 2100N Turbidimeter (HACH, Loveland, CO). Bulk water samples for microbiological analyses
127 (up to 5 L) were dechlorinated with sodium thiosulfate (Na₂S₂O₃) immediately after sample
128 collection and transported to the laboratory on ice.

129 After each sensor probe was dismantled from the water pipe, biofilms on the material
130 surfaces were collected by either scraping (for scaling) or swabbing using sterile cell scrapers or
131 cotton swabs, respectively. The sampled surface area (cm²) was measured (see section 2.1 for
132 specific values) to normalize microbial counts and calculate microbial surface density
133 (copies/cm²).

134 *2.3. Sample processing*

135 The dechlorinated bulk water samples (1 to 4 L of up to 5 L collected) were filtered through
136 the Isopore™ membrane filters (polycarbonate, pore size 0.2 µm, diameter 47 mm, cat. no.
137 GTTP04700; Millipore, Billerica, MA), and the filters were stored at -20°C for DNA extraction.
138 Heterotrophic plate count (HPC) numbers in the dechlorinated bulk water samples were
139 determined using R2A agar plates with an incubation at 20°C for 7 days (Reasoner, 2004). The
140 scrapings and swabs were suspended in sterile 1× phosphate-buffered saline (PBS), and biofilm
141 suspensions were prepared by vortexing. An aliquot of this biofilm suspension was used for
142 bacterial culture assays, and the rest of the suspension was stored at -20°C for DNA extraction.

143 *2.4. DNA extraction*

144 Total DNA was extracted from the filters and biofilm suspensions using the PowerWater® and

145 PowerBiofilm[®] DNA Isolation Kits (MO BIO Laboratories, Carlsbad, CA), respectively,
146 according to the manufacturer's instructions with slight modifications. Specifically, for the
147 biofilm samples 15 μ L of Proteinase K (Qiagen, Hilden, Germany) was added to the bead tube
148 after the bead-beating step and incubated at 65°C for 30 minutes to increase the yield of
149 eukaryotic DNA from biofilms.

150 *2.5. Droplet digital polymerase chain reaction (ddPCR)*

151 TaqMan-based ddPCR assays for total bacteria, total archaea, *Mycobacterium* spp., AOB,
152 *Nitrospira*-like NOB, *Gallionella* spp., cyanobacteria, and internal amplification control (murine
153 norovirus plasmid DNA, pMNV) were performed with a QX200[™] Droplet Digital[™] PCR
154 System (Bio-Rad, Pleasanton, CA). Reaction mixtures (20 μ L) consisted of 10 μ L of 1 \times
155 ddPCR[™] Supermix for Probes (Bio-Rad), forward and reverse primers and probe(s), and 2.0 μ L
156 of DNA template. The sequences of primers and probes are shown in Table S1 in the Supporting
157 information. The reaction mixture was mixed with droplet generation oil (20 μ L mixture and 70
158 μ L oil) via microfluidics in the QX200[™] Droplet Generator (Bio-Rad). The water-in-oil droplets
159 were transferred to a standard 96-well PCR plate and subjected to PCR amplification (ramping
160 speed at 2.5°C s⁻¹) on a C1000 Touch[™] Thermal Cycler (Bio-Rad). Upon completion of PCR, the
161 plate was transferred to a QX200[™] Droplet Reader (Bio-Rad) for automatic measurement of
162 fluorescent reading in each droplet in each well. A clear separation in terms of fluorescent
163 intensity was obtained between positive and negative droplets (Figure S3). Observed recovery
164 efficiency of internal control pMNV was >90%, suggesting no substantial inhibition in any of the
165 samples, except for S1 sample that showed 76% recovery (Figure S4). To minimize
166 contamination during the DNA extraction and ddPCR processes, DNA extraction and ddPCR
167 reagent preparation were performed in separate rooms. No template control (NTC) was included
168 in all ddPCR runs, and no amplification was observed in any NTC reactions.

169 *2.6. 16S rRNA gene amplicon sequencing and bioinformatics analysis*

170 A subset of the samples (a total of 12 samples [eight biofilm samples and four water
171 samples], collected from different substrata in S10, S11, S14, S15) was used for 16S rRNA gene
172 amplicon sequencing analysis. DNA concentrations in DNA extracts were determined by Qubit®
173 fluorometer (Thermo Fisher Scientific, Waltham, MA), according to the manufacturer's protocol.
174 Both bacterial and archaeal 16S rRNA genes were PCR-amplified using the universal primers
175 926wF and 1392R targeting the V6-V8 regions (Mason et al., 2012). The PCR amplicons were
176 sequenced with the Illumina MiSeq platform, a next-generation sequencer, with 300PE reads. The
177 raw reads were quality trimmed, primers and adapters were removed using cutadapt-1.8.1. All
178 data processing was conducted using QIIME 1.9.1 pipeline with Silva 16S rDNA database (>97%
179 identity level). In order to account for observed differences in sequencing depth per sample, the
180 operational taxonomic unit (OTU) abundance was rarefied to the lowest number of sequences in
181 a sample.

182 *2.7. Statistical analyses*

183 Two-way analysis of variance (ANOVA) and Tukey-Kremer's post-hoc multiple comparison
184 were performed within the R statistical computing environment (<http://www.r-project.org>) and
185 Microsoft Excel for Mac 2018 (Microsoft Corp., Redmond, WA), respectively, to investigate
186 whether the prokaryotic gene densities (\log_{10} copy numbers/cm²) were statistically different
187 between sampling sites and substratum types. Differences were considered statistically different
188 if the resultant *P*-value was 0.05 or lower. The statistical package PRIMER-PERMANOVA was
189 used for multivariate statistical analysis. The OTU abundance matrix was square-root
190 transformed and a Bray-Curtis resemblance matrix was used for further analysis.

191 *2.8. Nucleotide sequence accession numbers*

192 The raw sequencing reads were submitted to the sequence read archive (SRA) and can be
193 retrieved via the DNA Data Bank of Japan (DDBJ) accession number DRA009881.

194

195 **3. Results**

196 *3.1. Water quality*

197 Bulk water samples were available at 14 of the 17 study sites across two zones of the DWDS.
198 Water quality parameters measured in the bulk water samples are summarized in Table 1. The
199 DWDS is located in a tropical area, with high ambient water temperature ranging from 28.7 °C to
200 30.3 °C, and pH ranged from 6.89 to 7.74 without a clear relationship with other parameters.
201 There was a strong contrast in residual total chlorine levels and HPC between the two zones.
202 Throughout Zone 1, adequate concentrations of total residual chlorine (1.4 – 2.0 mg/L: range for
203 10 sites) are maintained and there were correspondingly low HPC counts (2.5 CFU/mL or less:
204 range for 11 sites), whereas Zone 2 samples showed much lower levels of total residual chlorine
205 (0.2 – 0.35 mg/L: range for 2 sites) and relatively higher HPC counts (8.5 – 11.5 CFU/mL: range
206 for 2 sites). Although the numbers of samples from each zone were limited, this result
207 demonstrates the presence of higher levels of heterotrophic bacteria in DWDS sections with
208 lower residual disinfectant levels associated with higher water age.

209 The abundance of prokaryotic genome copies in bulk water samples was determined by
210 target-specific ddPCR (Table 1). Bacterial and archaeal 16S rRNA genes were detected with the
211 highest copy numbers at S14 (1.51×10^6 and 2.79×10^4 copies/L, respectively). Bacterial 16S
212 rRNA genes (mean 1.10×10^5 copies/L) were always more abundant than archaeal 16S rRNA
213 genes (1.12×10^3 copies/L) with statistically significant difference ($P < 0.01$, *t*-test).

214 *Mycobacterium* spp., AOB, and Cyanobacteria were also detected from all water samples with
215 mean gene copy numbers of 2.69×10^4 , 1.23×10^4 , and 1.05×10^3 copies/L, respectively. The
216 sampling locations did not seem to impact the absolute abundance of these bacterial members in
217 bulk water samples as determined by ddPCR.

218 *3.2. Prokaryotic genomes in biofilm samples*

219 Abundance of prokaryotic genome copies in a total of 52 biofilm samples collected from four

220 different types of substratum (brass, SS, PVC, and POM) was determined by ddPCR (Table 2).
221 Biofilm age (i.e., duration of sensor operation) varied from 6 to 18 months in both zones.
222 Bacterial 16S rRNA gene was detected from all the biofilm samples with densities of up to $1.05 \times$
223 10^6 copies/cm². Statistical comparison of bacterial 16S rRNA gene densities (\log_{10} copies/cm²)
224 between different substratum types demonstrated that bacterial 16S rRNA gene copy numbers on
225 brass surface were significantly lower than those on other materials ($P < 0.05$). Whereas, the
226 comparison of bacterial 16S rRNA gene copy numbers between different sites identified no
227 statistically significant difference among sites ($P > 0.05$) despite the difference in biofilm age,
228 suggesting that accumulation of bacteria on sensor surface reached equilibrium within 6 months
229 of operation.

230 The archaeal 16S rRNA gene was always less abundant than the bacterial 16S rRNA gene,
231 but exhibited similar tendencies in terms of differences between substratum types and sampling
232 sites. For example, the archaeal 16S rRNA gene was less frequently detected on brass surface (3
233 out of 11, 27%) than on other substratum types (94% of SS, 100% of PVC, and 89% of POM
234 samples). *Mycobacterium* spp. were also less frequently detected on brass surfaces (8 out of 11,
235 73%) than on other substratum types (100%). The density of *Mycobacterium* spp. was close to
236 that of total bacteria based on 16S rRNA gene copy numbers, which was more notable in Zone 1
237 than in Zone 2 (Table 2). This result suggested that, in Zone 1, *Mycobacterium* spp. comprised a
238 significant portion of the bacterial population in biofilms, but this was not the case in Zone 2.
239 AOB were also detected in all biofilm samples at relatively high gene copy numbers, and at
240 lowest densities on brass surfaces. Cyanobacteria was generally less abundant than
241 *Mycobacterium* spp. and AOB.

242 Overall, densities of prokaryotic genome copies on brass surfaces tended to be lower than on
243 other substratum types, while there was no clear relationship with biofilm age between 6 and 18
244 months. We also noted that the trends in microbial abundance in biofilm samples were similar to

245 those in bulk water, with bacterial 16S rRNA gene being the most abundant, followed by
246 *Mycobacterium* spp. and AOB, and archaeal 16S rRNA and cyanobacteria being less abundant
247 than other microbial groups.

248 3.3. 16S rRNA gene amplicon sequencing analysis

249 The prokaryotic community composition in the biofilm and water samples was determined
250 for a total of 12 samples collected from four sites (S10, S11, S14, S15), based on 16S rRNA gene
251 amplicon sequencing using the Illumina MiSeq platform. After quality filtering, 288,642 to
252 432,154 high quality reads were obtained per sample (Table 3). The rarefaction curves for all
253 samples had reached plateaus (Figure S5), suggesting that the sequencing depth was adequate to
254 capture most of the diversity within the microbial communities in each sample. There was no
255 remarkable difference in richness and diversity indices between sample types or sampling sites
256 (Table 3). Figure 1 shows relative abundances in total sequencing reads (%) of prokaryotic
257 (including *Archaea* and *Bacteria*) 16S rRNA gene amplicons in biofilms on SS surfaces as well
258 as in water samples. *Archaea* were much less abundant than *Bacteria* (relative abundance of up to
259 4.2 % in total reads; included in “Others”), which is consistent with the results of ddPCR absolute
260 quantification (Table 2). In Zone 1 (S10 and S11), the genus *Mycobacterium* and the family
261 *Nitrosomonadaceae* (genus unassigned) were abundant in both biofilm and local water samples.
262 The family *Nitrosomonadaceae* comprises two genera, *Nitrosomonas* and *Nitrospira*, both of
263 whose cultivated representatives are chemolithoautotrophic ammonia oxidizers (Prosser et al.,
264 2014). In contrast, the genus *Nitrospira*, which is represented by aerobic chemolithoautotrophic
265 NOB (Daims and Wagner, 2018), was dominant in Zone 2 (S14 and S15) samples.

266 Non-metric multidimensional scaling (nMDS) plots, which produced an ordination based on
267 the Bray-Curtis dissimilarity matrix, indicate a dissimilarity in microbial community structure in
268 samples from Zone 1 (S10 and S11) and Zone 2 (S14 and S15) (Figure 2). These two zones had
269 contrasting hydraulic and water quality characteristics, such as water age and residual disinfectant

270 levels, as described above (Table 1). Within each zone, the physical phase (biofilm vs bulk water)
271 exerted greater influence on microbial communities than sampling locations (Figure 2).

272

273 **4. Discussion**

274 In the present study, we examined microbial communities in biofilm and water samples
275 collected from the WaterWiSe sensors inserted in water pipes of a full-scale operational DWDS.
276 Our strategy enabled collection of samples from the sensors installed at different locations within
277 the DWDS with varying water age and residual chlorine.

278 The abundance of prokaryotic genome copies was determined by ddPCR. This allowed direct
279 comparison of microbial abundance among different microbial groups in each sample. Bacteria
280 were always more abundant than archaea in both bulk water and biofilm samples, which was also
281 supported by 16S rRNA gene amplicon sequencing analysis. In addition to bacterial and archaeal
282 16S rRNA genes, *Mycobacterium* spp., AOB, and Cyanobacteria were selected as detection
283 targets, because their presence in DWDS and significance to drinking water quality have been
284 reported previously (Haig et al., 2018; Lipponen et al., 2004; Shaw et al., 2015; Zhang et al.,
285 2017). In agreement with the previous studies, these bacterial groups were frequently detected at
286 high abundance; for example, densities of *Mycobacterium* spp. as well as bacterial 16S rRNA
287 genes in bulk water were comparable to those reported in a previous study based on quantitative
288 PCR (Haig et al., 2018).

289 It has been reported that the characteristics of the substratum material may greatly influence
290 formation and growth of biofilms in DWDS (Niquette et al., 2000; Wang et al., 2012). The
291 WaterWiSe sensors were composed of multiple parts with different materials (i.e., brass, SS,
292 PVC, and POM), which provided a unique opportunity to investigate the density of
293 microorganisms depending on material types serving as a substrate for biofilms in real DWDS.
294 One of the limitations of this study is that only one biofilm sample was collected from each

295 surface type of each sensor, although the density and composition of biofilms on surfaces can
296 greatly vary due to heterogeneity in drinking water biofilms (Neu et al., 2019). The ddPCR
297 results demonstrated that densities of microbial genome copies on brass were substantially lower
298 than on other materials. This is probably because brass consists of copper and zinc, both of which
299 exhibit antimicrobial properties (Espírito Santo et al., 2008; McDevitt et al., 2011). Other
300 materials studied, especially SS and PVC, are frequently used as pipe material, and their ability to
301 support drinking water biofilm has been investigated previously (Jang et al., 2011). Our results
302 indicated that these materials support colonization and growth of biofilms in water pipes even in
303 the DWDS sections where an adequate residual disinfectant level is maintained.

304 Prokaryotic 16S rRNA gene sequencing analysis using the Illumina MiSeq platform was
305 performed to gain further insights into the impact of environmental factors to microbial
306 composition. Due to resource constraints, biological and technical replicates could not be
307 included in the sampling design (i.e., $n = 1$ for each sampling point) and only a subset of samples
308 was subjected to 16S rRNA gene sequencing analysis, which is one of the major limitations of
309 this study. In selecting the subset (12 out of a total of 66 samples), consideration was given to a
310 comparison of microbial composition between different physical phases (water and biofilm),
311 zones (S10 and S11 in zone 1 and S14 and S15 in zone 2), and substratum types (SS, PVC, and
312 POM). The nMDS analysis showed that microbial composition was primarily impacted by zone,
313 rather than physical phase or substratum type. Because the two zones were characterized by
314 contrasting residual disinfectant levels and water age, these parameters could be the major factors
315 affecting microbial composition in DWDS. Other parameters, such as age of biofilm on sensors
316 (Table 2), pipe diameter, velocity, and pipe material (Table S2), differed among the studied sites,
317 but similarities in microbial composition were observed within a zone rather than between zones
318 (Figure 2). Although a number of previous studies reported the distinctions in microbial
319 compositions between planktonic and biofilm communities in DWDSs (Douterelo et al., 2013;

320 Ling et al., 2016), our nMDS analysis indicated that microbial communities in water and biofilm
321 samples collected from the same site in the present study were similar. This inconsistency might
322 be derived from the age of biofilms and shear stress. Most of the previous studies examined
323 mature biofilms developed on pipe walls or water meters with presumably limited shear stress,
324 whereas our biofilm samples were relatively immature (i.e., 6 to 18 months old) and collected
325 from the surface of the sensors inserted in the center of water pipe with greater shear stress due to
326 higher water velocity.

327 Taxa identified in samples with high levels of a disinfectant like monochloramine include
328 species that are resistant to or tolerant of disinfectants. The genus *Mycobacterium* predominated
329 in Zone 1 where the residual disinfectant level was relatively high. Previous studies indicated that
330 chloramine is less effective than chlorine against *Mycobacterium* spp. and they are among the
331 most dominant members of the microbial community in chloraminated DWDS (Donohue et al.,
332 2015; Gomez-Smith et al., 2015). In Zone 2, relatively low residual disinfectant levels may have
333 allowed growth of other bacterial species including those susceptible to monochloramine. The
334 observed difference in microbial composition between the two zones could be primarily due to
335 different residual chloramine levels, because some previous studies suggested that the
336 disinfection pressure of chloramine substantially impacted microbial community structure in
337 DWDS (Cruz et al., 2020; Mi et al., 2015; Waak et al., 2019).

338 The other predominant taxon in Zone 1 was the family *Nitrosomonadaceae*, which is
339 represented by lithoautotrophic AOB that oxidize ammonia to nitrite (Prosser et al., 2014).
340 Although the concentration of ammonia was not measured in this study, free ammonia is
341 inevitably present in chloraminated drinking water as a consequence of the process to generate
342 monochloramine. The predominance of *Nitrosomonadaceae* in Zone 1 indicates biological
343 ammonia oxidation activities owing to the presence of free ammonia in the fresh chloraminated
344 water. The abundance of AOB was also demonstrated by ddPCR quantification where AOB 16S

345 rRNA genes were detected in all samples with high numbers of up to 1.55×10^5 copies/cm² in
346 biofilms and 9.07×10^4 copies/L in bulk water. Few studies have investigated the occurrence of
347 AOA in drinking water systems (Kasuga et al., 2010; Nagymáté et al., 2016; Van Der Wielen et
348 al., 2009), and it was reported that the number of AOA could exceed the number of AOB in
349 drinking water (Van Der Wielen et al., 2009). Our SYBR Green-based qPCR screening of AOB
350 and AOA *amoA* genes demonstrated that the AOB *amoA* gene is more widely distributed than
351 AOA *amoA* gene in this DWDS (Table S4). These results suggest that ammonia-oxidizing
352 activities of AOB contributing to nitrification were distributed across the DWDS.

353 There is a strong contrast in the predominance of the genus *Nitrospira* between the two zones
354 with higher relative abundance in Zone 2. *Nitrospira* is known as NOB and plays pivotal roles in
355 nitrification by oxidizing nitrite to nitrate (Daims and Wagner, 2018). The results suggest the
356 availability of nitrite produced as a result of ammonia oxidization and prominent nitrite
357 oxidization activities of *Nitrospira* in Zone 2, which was also implied in a recent study
358 investigating biofilm communities on pipe walls of a tropical DWDS (Cruz et al., 2020).

359 Nitrification, a biological oxidation of ammonia to nitrite by AOB and/or AOA and further to
360 nitrate by NOB, is a major issue for chloraminated DWDS (Zhang et al., 2009). This is because
361 the intermediate nitrite can also be oxidized by chloramine in drinking water, which consumes
362 chloramine and results in bacterial growth. In the present study, we observed the presence of
363 AOB across the DWDS as well as decreased total residual chlorine level and increased HPC
364 numbers in bulk water and abundance of *Nitrospira* in Zone 2, which collectively suggests the
365 occurrence of nitrification in the studied DWDS. Our observations on the distribution of nitrifiers
366 within the DWDS suggested that ammonia-oxidizers produce nitrite in Zone 1, which enhances
367 residual monochloramine decay, whereas in Zone 2, nitrite is oxidized by *Nitrospira* and
368 produces nitrate. One of the major limitations of this study is a lack of measurements of
369 ammonia, nitrite, and nitrate concentrations to confirm this process. Another limitation is that

370 very small numbers of samples were available from Zone 2 (i.e., 2 sites) due to limited sampling
371 access within the operational DWDS. Nonetheless, our results are consistent at sites S14 and S15
372 in Zone 2 and the data from Zone 2 appear as outliers for the statistics on Zone 1. We are
373 therefore quite confident of our findings, despite of the practical limitation on sampling access.

374

375 **5. Conclusions**

376 The present study provides novel information on the abundance and composition of
377 prokaryotes present in biofilms and water in a full-scale operational DWDS. Our main
378 conclusions are:

- 379 • The trends in ddPCR-based microbial abundance in biofilm samples were similar to those in
380 bulk water, with bacterial 16S rRNA gene being the most abundant, followed by
381 *Mycobacterium* spp. and AOB, and archaeal 16S rRNA and cyanobacteria being less
382 abundant than other microbial groups.
- 383 • Densities of prokaryotic genome copies on brass surface tended to be lower than on other
384 substrate types (SS, PVC, and POM).
- 385 • *Mycobacterium* and AOB species were dominant in Zone 1 with low water age and sufficient
386 residual monochloramine, whereas *Nitrospira* species dominated in Zone 2 with higher water
387 age and depleted monochloramine level. This result suggests the occurrence of nitrification in
388 the studied DWDS.
- 389 • Microbial community structure was primarily affected by differences in zones characterized
390 by contrasting hydraulic and water quality characteristics, such as water age and residual
391 disinfectant levels. Within each zone, the physical phase (biofilm vs bulk water) had a greater
392 influence on microbial communities than sampling location.

393

394

395
396
397
398
399
400
401
402
403
404

ACKNOWLEDGMENTS

This work was partly supported by funding from the Singapore National Research Foundation and the Singapore-MIT Alliance for Research and Technology (SMART), through the Center for Environmental Sensing and Modeling (CENSAM) research program. This work was also supported by the Singapore National Research Foundation and Ministry of Education under the Research Centre of Excellence Programme. The authors are very grateful to Visenti Pte. Ltd. for their support and collaboration in this research. The authors also would like to thank Prof. Karina Yew-Hoong Gin and Ms. Kalaivani Mani at the National University of Singapore for their laboratory and technical assistance.

REFERENCES

- 405
- 406 Abbaszadegan, M., Yi, M., Alum, A., 2015. Stimulation of 2-methylisoborneol (MIB) production
407 by actinomycetes after cyclic chlorination in drinking water distribution systems. *J. Env. Sci.*
408 *Heal. A Tox Hazard Subst Env. Eng* 50, 365–371.
- 409 Allen, M., Preis, A., Iqbal, M., Srirangarajan, S., Lim, H.B., Girod, L., Whittle, A.J., 2011. Real-
410 time in-network distribution system monitoring to improve operational efficiency. *J. Am.*
411 *Water Work. Assoc.* 103, 63–75.
- 412 Cruz, M.C., Woo, Y., Flemming, H.C., Wuertz, S., 2020. Nitrifying niche differentiation in biofilms
413 from full-scale chloraminated drinking water distribution system. *Water Res.* 176.
414 <https://doi.org/10.1016/j.watres.2020.115738>
- 415 Daims, H., Wagner, M., 2018. Nitrospira. *Trends Microbiol.* 26, 462–463.
416 <https://doi.org/10.1016/j.tim.2018.02.001>
- 417 Donohue, M.J., Mistry, J.H., Donohue, J.M., Oconnell, K., King, D., Byran, J., Covert, T., Pfaller,
418 S., 2015. Increased frequency of nontuberculous mycobacteria detection at potable water taps
419 within the United States. *Environ. Sci. Technol.* 49, 6127–6133.
420 <https://doi.org/10.1021/acs.est.5b00496>
- 421 Douterelo, I., Boxall, J.B., Deines, P., Sekar, R., Fish, K.E., Biggs, C.A., 2014. Methodological
422 approaches for studying the microbial ecology of drinking water distribution systems. *Water*
423 *Res.* 65, 134–156. <https://doi.org/10.1016/j.watres.2014.07.008>
- 424 Douterelo, I., Dutilh, B.E., Arkhipova, K., Calero, C., Husband, S., 2020. Microbial diversity,
425 ecological networks and functional traits associated to materials used in drinking water
426 distribution systems. *Water Res.* 173, 115586. <https://doi.org/10.1016/j.watres.2020.115586>
- 427 Douterelo, I., Sharpe, R.L., Boxall, J.B., 2013. Influence of hydraulic regimes on bacterial
428 community structure and composition in an experimental drinking water distribution system.

429 Water Res. 47, 503–516. <https://doi.org/10.1016/j.watres.2012.09.053>

430 Espírito Santo, C., Taudte, N., Nies, D.H., Grass, G., 2008. Contribution of copper ion resistance
431 to survival of *Escherichia coli* on metallic copper surfaces. *Appl. Environ. Microbiol.* 74, 977–
432 986. <https://doi.org/10.1128/AEM.01938-07>

433 Fish, K.E., Collins, R., Green, N.H., Sharpe, R.L., Douterelo, I., Osborn, A.M., Boxall, J.B., 2015.
434 Characterisation of the physical composition and microbial community structure of biofilms
435 within a model full-scale drinking water distribution system. *PLoS One* 10, 1–22.
436 <https://doi.org/10.1371/journal.pone.0115824>

437 Gomez-Alvarez, V., Schrantz, K.A., Pressman, J.G., Wahman, D.G., 2014. Biofilm community
438 dynamics in bench-scale annular reactors simulating arrestment of chloraminated drinking
439 water nitrification. *Environ. Sci. Technol.* 48, 5448–5457. <https://doi.org/10.1021/es5005208>

440 Gomez-Smith, C.K., Lapara, T.M., Hozalski, R.M., 2015. Sulfate reducing bacteria and
441 mycobacteria dominate the biofilm communities in a chloraminated drinking water
442 distribution system. *Environ. Sci. Technol.* 49, 8432–8440.
443 <https://doi.org/10.1021/acs.est.5b00555>

444 Haig, S.J., Kotlarz, N., Lipuma, J.J., Raskin, L., 2018. A high-throughput approach for
445 identification of nontuberculous mycobacteria in drinking water reveals relationship between
446 water age and *Mycobacterium avium*. *MBio* 9, 1–13. <https://doi.org/10.1128/mBio.02354-17>

447 Hong, P.-Y., Hwang, C., Ling, F., Andersen, G.L., LeChevallier, M.W., Liu, W.-T., 2010.
448 Pyrosequencing analysis of bacterial biofilm communities in water meters of a drinking water
449 distribution system. *Appl. Environ. Microbiol.* 76, 5631–5635.
450 <https://doi.org/10.1128/AEM.00281-10>

451 Jang, H.-J., Choi, Y.J., Ka, J.O., 2011. Effects of diverse water pipe materials on bacterial
452 communities and water quality in the annular reactor. *J. Microbiol. Biotechnol.* 21, 115–123.

453 <https://doi.org/10.4014/jmb.1010.10012>

454 Kasuga, I., Nakagaki, H., Kurisu, F., Furumai, H., 2010. Predominance of ammonia-oxidizing
455 archaea on granular activated carbon used in a full-scale advanced drinking water treatment
456 plant. *Water Res.* 44, 5039–5049. <https://doi.org/10.1016/j.watres.2010.07.015>

457 Kelly, J.J., Minalt, N., Culotti, A., Pryor, M., Packman, A., 2014. Temporal variations in the
458 abundance and composition of biofilm communities colonizing drinking water distribution
459 pipes. *PLoS One* 9. <https://doi.org/10.1371/journal.pone.0098542>

460 Koskinen, R., Tali-Vehmas, Kämpfer, P., Laurikkala, M., Tsitko, I., Kostyal, E., Atroshi, F.,
461 Salkinoja-Salonen, M., 2000. Characterization of *Sphingomonas* isolates from Finnish and
462 Swedish drinking water distribution systems. *J. Appl. Microbiol.* 89, 687–696.
463 <https://doi.org/10.1046/j.1365-2672.2000.01167.x>

464 Lee, W.H., Wahman, D.G., Bishop, P.L., Pressman, J.G., 2011. Free chlorine and monochloramine
465 application to nitrifying biofilm: Comparison of biofilm penetration, activity, and viability.
466 *Environ. Sci. Technol.* 45, 1412–1419. <https://doi.org/10.1021/es1035305>

467 Ling, F., Hwang, C., LeChevallier, M.W., Andersen, G.L., Liu, W.T., 2016. Core-satellite
468 populations and seasonality of water meter biofilms in a metropolitan drinking water
469 distribution system. *ISME J.* 10, 582–595. <https://doi.org/10.1038/ismej.2015.136>

470 Lipponen, M.T.T., Martikainen, P.J., Vasara, R.E., Servomaa, K., Zacheus, O., Kontro, M.H., 2004.
471 Occurrence of nitrifiers and diversity of ammonia-oxidizing bacteria in developing drinking
472 water biofilms. *Water Res.* 38, 4424–4434. <https://doi.org/10.1016/j.watres.2004.08.021>

473 Liu, G., Verberk, J.Q.J.C., Van Dijk, J.C., 2013. Bacteriology of drinking water distribution
474 systems: an integral and multidimensional review. *Appl. Microbiol. Biotechnol.* 97, 9265–
475 9276. <https://doi.org/10.1007/s00253-013-5217-y>

476 Liu, G., Zhang, Y., Liu, X., Hammes, F., Liu, W.T., Medema, G., Wessels, P., van der Meer, W.,

477 2020. 360-Degree Distribution of Biofilm Quantity and Community in an Operational
478 Unchlorinated Drinking Water Distribution Pipe. *Environ. Sci. Technol.* 54, 5619–5628.
479 <https://doi.org/10.1021/acs.est.9b06603>

480 Liu, S., Gunawan, C., Barraud, N., Rice, S.A., Harry, E.J., Amal, R., 2016. Understanding,
481 monitoring, and controlling biofilm growth in drinking water distribution systems. *Environ.*
482 *Sci. Technol.* 50, 8954–8976. <https://doi.org/10.1021/acs.est.6b00835>

483 Lührig, K., Canbäck, B., Paul, C.J., Johansson, T., Persson, K.M., Rådström, P., 2015. Bacterial
484 Community Analysis of Drinking Water Biofilms in Southern Sweden. *Microbes Environ.*
485 *Environ.* 30, 99–107. <https://doi.org/10.1264/jsme2.me14123>

486 Mason, O.U., Hazen, T.C., Borglin, S., Chain, P.S.G., Dubinsky, E.A., Fortney, J.L., Han, J.,
487 Holman, H.-Y.N., Hultman, J., Lamendella, R., Mackelprang, R., Malfatti, S., Tom, L.M.,
488 Tringe, S.G., Woyke, T., Zhou, J., Rubin, E.M., Jansson, J.K., 2012. Metagenome,
489 metatranscriptome and single-cell sequencing reveal microbial response to Deepwater
490 Horizon oil spill. *ISME J.* 6, 1715–1727. <https://doi.org/10.1038/ismej.2012.59>

491 McDevitt, C.A., Ogunniyi, A.D., Valkov, E., Lawrence, M.C., Kobe, B., McEwan, A.G., Paton,
492 J.C., 2011. A molecular mechanism for bacterial susceptibility to Zinc. *PLoS Pathog.* 7,
493 e1002357. <https://doi.org/10.1371/journal.ppat.1002357>

494 Mi, Z., Dai, Y., Xie, S., Chen, C., Zhang, X., 2015. Impact of disinfection on drinking water biofilm
495 bacterial community. *J. Environ. Sci. (China)* 37, 200–205.
496 <https://doi.org/10.1016/j.jes.2015.04.008>

497 Nagymáté, Z., Homonnay, Z.G., Márialigeti, K., 2016. Investigation of Archaeal and Bacterial
498 community structure of five different small drinking water networks with special regard to the
499 nitrifying microorganisms. *Microbiol. Res.* 188–189, 80–89.
500 <https://doi.org/10.1016/j.micres.2016.04.015>

501 Neu, L., Proctor, C.R., Walser, J.C., Hammes, F., 2019. Small-scale heterogeneity in drinking water
502 biofilms. *Front. Microbiol.* 10, 1–14. <https://doi.org/10.3389/fmicb.2019.02446>

503 Niquette, P., Servais, P., Savoie, R., 2000. Impacts of pipe materials on densities of fixed bacterial
504 biomass in a drinking water distribution system. *Water Res.* 34, 1952–1956.
505 [https://doi.org/10.1016/S0043-1354\(99\)00307-3](https://doi.org/10.1016/S0043-1354(99)00307-3)

506 Norton, C.D., LeChevallier, M.W., 1997. Chloramination: its effect on distribution system water
507 quality. *J. Am. Water Works Assoc.* 89, 66–77. <https://doi.org/10.1002/j.1551-8833.1997.tb08260.x>

509 Prosser, J.I., Head, I.M., Stein, L.Y., 2014. The Family Nitrosomonadaceae, in: Rosenberg, E.,
510 DeLong, E.F., Lory, S., Stackebrandt, E., Thompson, F. (Eds.), *The Prokaryotes: Alphaproteobacteria and Betaproteobacteria*. Springer Berlin Heidelberg, Berlin, Heidelberg,
511 pp. 901–918. https://doi.org/10.1007/978-3-642-30197-1_372

513 Reasoner, D.J., 2004. Heterotrophic plate count methodology in the United States. *Int. J. Food*
514 *Microbiol.* 92, 307–315. <https://doi.org/10.1016/j.ijfoodmicro.2003.08.008>

515 Rossman, L., 2000. EPANET 2 users manual [WWW Document]. U.S. Environ. Prot. Agency.

516 Schwake, D., Alum, A., Abbaszadegan, M., 2015. Impact of Environmental Factors on Legionella
517 Populations in Drinking Water. *Pathogens* 4, 269–282.
518 <https://doi.org/10.3390/pathogens4020269>

519 Seidel, C.J., McGuire, M.J., Summers, R.S., Via, S., 2005. Have utilities switched to chloramines?
520 *J. Am. Water Work. Assoc.* 97, 87–97. <https://doi.org/10.1002/j.1551-8833.2005.tb07497.x>

521 Shaw, J.L.A., Monis, P., Weyrich, L.S., Sawade, E., Drikas, M., Cooper, A.J., 2015. Using amplicon
522 sequencing to characterize and monitor bacterial diversity in drinking water distribution
523 systems. *Appl. Environ. Microbiol.* 81, 6463–6473. <https://doi.org/10.1128/AEM.01297-15>

524 Van Der Wielen, P.W.J.J., Voost, S., Van Der Kooij, D., 2009. Ammonia-oxidizing bacteria and
525 archaea in groundwater treatment and drinking water distribution systems. *Appl. Environ.*
526 *Microbiol.* 75, 4687–4695. <https://doi.org/10.1128/AEM.00387-09>

527 Waak, M.B., Hozalski, R.M., Hallé, C., Lapara, T.M., 2019. Comparison of the microbiomes of
528 two drinking water distribution systems - With and without residual chloramine disinfection.
529 *Microbiome* 7, 1–14. <https://doi.org/10.1186/s40168-019-0707-5>

530 Wang, H., Masters, S., Hong, Y., Stallings, J., Falkinham, J.O., Edwards, M.A., Pruden, A., 2012.
531 Effect of disinfectant, water age, and pipe material on occurrence and persistence of
532 *Legionella*, mycobacteria, *Pseudomonas aeruginosa*, and two amoebas. *Environ. Sci. Technol.*
533 46, 11566–74. <https://doi.org/10.1021/es303212a>

534 Watson, C.L., Owen, R.J., Said, B., Lai, S., Lee, J. V., Surman-Lee, S., Nichols, G., 2004. Detection
535 of *Helicobacter pylori* by PCR but not culture in water and biofilm samples from drinking
536 water distribution systems in England. *J. Appl. Microbiol.* 97, 690–698.
537 <https://doi.org/10.1111/j.1365-2672.2004.02360.x>

538 Zhang, Y., Kitajima, M., Whittle, A.J., Liu, W.T., 2017. Benefits of genomic insights and CRISPR-
539 Cas signatures to monitor potential pathogens across drinking water production and
540 distribution systems. *Front. Microbiol.* 8, 1–15. <https://doi.org/10.3389/fmicb.2017.02036>

541 Zhang, Y., Love, N., Edwards, M., 2009. Nitrification in drinking water systems. *Crit. Rev. Environ.*
542 *Sci. Technol.* 39, 153–208. <https://doi.org/10.1080/10643380701631739>

543

1 **Table 1.** Water quality parameters and abundance of prokaryotic genome copies in bulk water^a.

Zone	Site ID	Water quality parameters						Prokaryotic genome copies (copies/L)				
		Water age (h) ^b	Temp. (°C)	pH	Total chlorine (mg/L)	Free chlorine (mg/L)	HPC ^c (CFU/ml)	<i>Bacteria</i>	<i>Archaea</i>	<i>Mycobacterium</i> spp.	AOB	Cyanobacteria
1	S1	16.0	28.7	7.36	2.0	<0.1	<1	5.30×10 ⁴	4.75×10 ²	1.83×10 ⁴	1.41×10 ⁴	2.10×10 ²
	S2	12.3	NA	NA ^c	NA	NA	NA	NA	NA	NA	NA	NA
	S3	7.9	28.8	6.89	1.9	<0.1	<1	4.65×10 ⁵	2.70×10 ³	1.61×10 ⁵	9.07×10 ⁴	3.90×10 ³
	S4	20.1	NA	NA	NA	NA	NA	NA	NA	NA	NA	NA
	S5	10.0	29.0	7.39	1.9	<0.1	2	4.68×10 ⁴	2.75×10 ²	1.89×10 ⁴	7.70×10 ³	3.65×10 ²
	S6	9.5	29.3	7.48	1.9	<0.1	1.5	6.12×10 ⁴	5.70×10 ²	1.91×10 ⁴	7.15×10 ³	7.00×10 ²
	S7	11.0	29.3	7.57	1.9	<0.1	NT ^d	1.46×10 ⁵	2.20×10 ²	7.90×10 ⁴	1.13×10 ⁴	1.28×10 ⁴
	S8	8.1	29.3	7.67	1.9	<0.1	1	3.12×10 ⁴	1.10×10 ³	9.15×10 ³	6.50×10 ³	2.55×10 ²
	S9	5.0	29.2	7.48	1.8	<0.1	<1	1.20×10 ⁵	4.73×10 ³	4.87×10 ⁴	1.14×10 ⁴	6.67×10 ²
	S10	3.1	29.1	7.51	1.9	<0.1	<1	3.04×10 ⁴	3.00×10 ²	1.89×10 ⁴	3.57×10 ³	2.98×10 ²
	S11	11.1	29.1	7.65	1.9	<0.1	<1	3.93×10 ⁴	3.43×10 ²	1.24×10 ⁴	6.03×10 ³	9.67×10 ²
	S12	7.8	29.2	7.43	1.4	<0.1	2	4.61×10 ⁴	6.33×10 ²	1.98×10 ⁴	9.13×10 ³	6.67×10 ²
	S13	12.4	NA	NA	NA	NA	NA	NA	NA	NA	NA	NA
	S16	13.9	30.0	7.53	NT	NT	2.5	2.47×10 ⁵	1.07×10 ⁴	4.73×10 ⁴	2.24×10 ⁴	1.43×10 ²
S17	17.2	29.1	7.27	NT	NT	1	4.67×10 ⁴	6.67×10 ²	2.05×10 ⁴	1.02×10 ⁴	1.40×10 ³	
2	S14	45.1	29.2	7.40	0.2	<0.1	8.5	1.51×10 ⁶	2.79×10 ⁴	2.46×10 ⁴	4.23×10 ⁴	1.57×10 ⁴
	S15	35.9	30.3	7.74	0.35	<0.1	11.5	1.09×10 ⁶	1.73×10 ³	2.67×10 ⁴	1.48×10 ⁴	6.47×10 ³
							Mean	1.20×10 ⁵	1.12×10 ³	2.69×10 ⁴	1.23×10 ⁴	1.05×10 ³

2 ^aOne bulk water sample (n = 1) was collected from each sampling site where the sample was available and analyzed once without
3 technical replicate.

4 ^b20-h average water age calculated with the EPANET hydraulic model.

5 ^c HPC, heterotrophic plate count; CFU, colony-forming units.

6 ^d NA, sample not available.

7 ^e NT, not tested.

8

1 **Table 2.** Abundance of prokaryotic genome copies in biofilm samples^a.

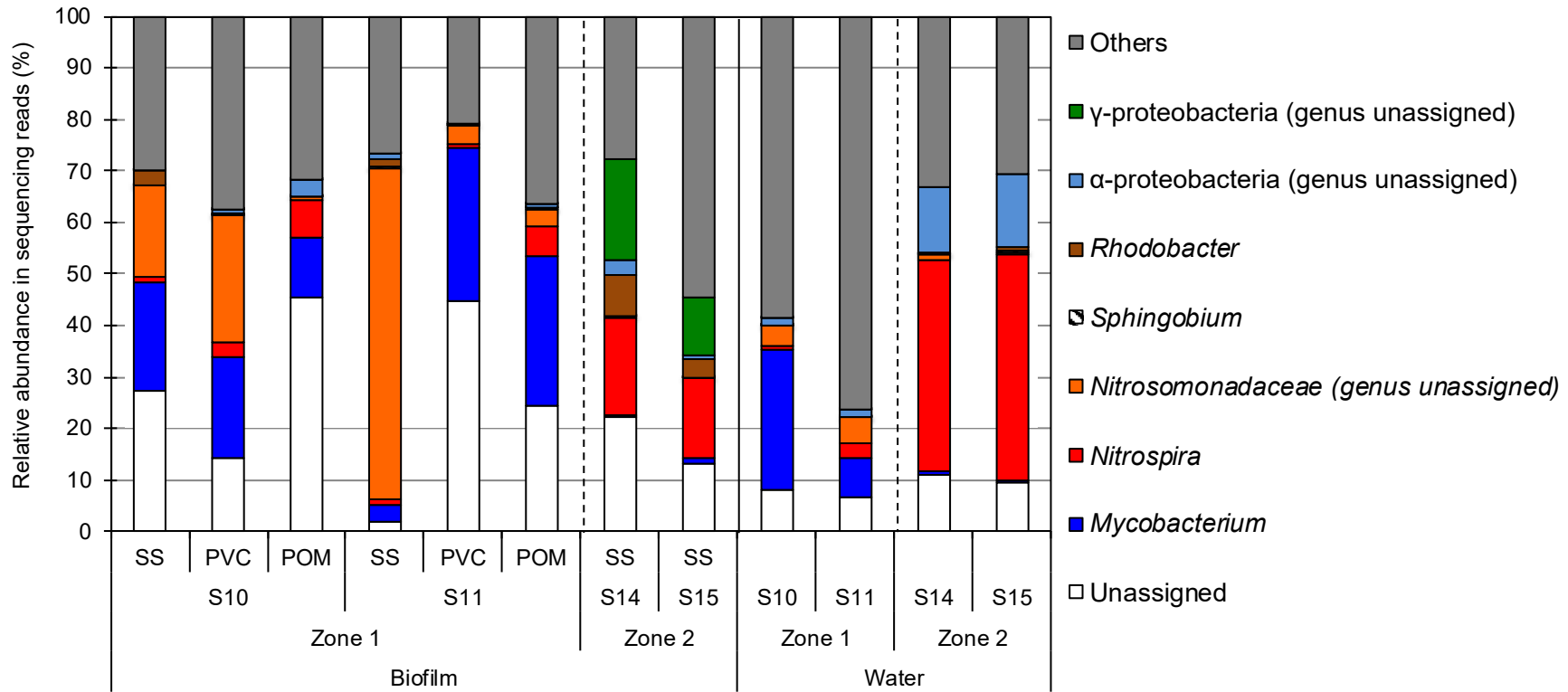
Zone	Site	Biofilm age (mo)	<i>Bacteria</i>				<i>Archaea</i>				<i>Mycobacterium</i> spp.				AOB				Cyanobacteria				
			Brass	SS ^b	PVC ^b	POM ^b	Brass	SS	PVC	POM	Brass	SS	PVC	POM	Brass	SS	PVC	POM	Brass	SS	PVC	POM	
1	S1	12	1.90	3.98	3.35	NA ^c	<0.09	1.67	1.50	NA	0.24	4.14	2.69	NA	1.84	2.93	2.50	NA	0.96	0.97	1.06	NA	
	S2	6	NA	3.47	NA	3.97	NA	0.06	NA	1.17	NA	3.19	NA	2.96	NA	2.47	NA	3.41	NA	1.44	NA	2.01	
	S3	12	3.97	4.64	3.88	NA	1.93	2.60	1.15	NA	3.07	3.75	3.39	NA	3.95	4.61	2.91	NA	1.54	2.15	0.88	NA	
	S4	10	NA	3.19	NA	4.89	NA	1.16	NA	0.94	NA	2.89	NA	3.46	NA	2.80	NA	3.42	NA	1.12	NA	2.17	
	S5	12	2.29	4.21	4.41	NA	<-0.11	1.49	1.87	NA	<-0.11	4.30	4.60	NA	1.66	3.58	3.25	NA	0.03	2.22	1.48	NA	
	S6	18	1.96	4.71	3.76	4.98	<-0.12	2.56	1.48	3.26	<-0.12	4.78	3.48	4.38	1.72	3.57	3.16	3.83	0.78	2.22	1.72	2.50	
	S7	6	4.45	4.37	4.60	NA	1.24	<0.61	0.32	NA	4.11	4.19	4.79	NA	3.33	4.04	2.69	NA	1.84	1.60	0.96	NA	
	S8	18	NA	4.70	3.70	4.41	NA	2.71	1.52	2.57	NA	3.06	3.00	3.17	NA	4.01	2.77	3.60	NA	2.02	1.26	2.03	
	S9	12	2.56	4.74	3.20	NA	<-0.02	1.81	0.34	NA	0.33	4.81	2.53	NA	1.14	3.42	2.39	NA	<-0.02	1.87	0.62	NA	
	S10	12	1.78	4.15	3.39	4.88	<-0.01	1.50	0.80	2.98	<-0.01	4.29	3.18	4.53	1.24	3.44	2.95	3.63	<-0.01	2.18	1.08	2.46	
	S11	6	2.03	4.71	3.98	3.87	<-0.04	1.85	1.14	0.49	1.26	3.88	4.24	3.88	1.52	4.70	2.73	2.70	<-0.04	2.56	0.72	0.76	
	S12	6	NA	5.63	4.40	4.43	NA	2.25	0.21	<0.11	NA	4.87	4.23	4.03	NA	4.91	3.63	3.63	NA	1.54	0.95	1.22	
	S13	6	NA	4.79	3.29	NA	NA	1.99	0.12	NA	NA	4.24	2.67	NA	NA	4.70	2.98	NA	NA	2.60	0.99	NA	
	S16	12	2.72	6.02	4.04	5.06	<0.06	2.32	1.22	2.98	1.84	4.13	3.30	3.58	2.22	4.85	2.96	3.49	<0.06	3.09	1.80	2.86	
	S17	6	NA	5.20	4.22	4.36	NA	1.69	1.25	2.09	NA	4.65	4.22	3.74	NA	5.19	3.56	3.89	NA	2.35	1.46	2.21	
	2	S14	18	4.09	5.62	3.98	NA	0.52	2.53	-0.07	NA	2.54	3.94	2.53	NA	2.91	4.30	2.49	NA	1.05	3.78	0.96	NA
		S15	12	2.48	5.19	4.88	NA	<0.01	1.33	0.86	NA	1.13	3.59	3.15	NA	1.98	3.48	4.35	NA	<0.01	3.37	1.40	NA
		Mean	2.66	4.67	3.94	4.54	1.23	1.85	0.91	2.06	1.81	4.04	3.47	3.75	2.14	3.94	3.02	3.51	1.03	2.18	1.16	2.02	
		SD	1.02	0.75	0.50	0.44	0.70	0.68	0.60	1.06	1.36	0.60	0.77	0.52	0.90	0.81	0.52	0.35	0.63	0.76	0.35	0.65	
		No. of positive (%)	11 (100)	17 (100)	15 (100)	9 (100)	3 (27)	16 (94)	15 (100)	8 (89)	8 (73)	17 (100)	15 (100)	9 (100)	11 (100)	17 (100)	15 (100)	9 (100)	6 (55)	17 (100)	15 (100)	9 (100)	

- 2 ^a Values are expressed in log₁₀ copies/cm². One biofilm sample (n = 1) was collected and analyzed from each surface type and analyzed
- 3 once without technical replicate.
- 4 ^b SS, stainless steel; PVC, polyvinyl chloride; POM, polyoxymethylene.
- 5 ^c NA, not available.

- 1 **Table 3.** Alpha diversity of microbial communities in biofilms on various surface materials
 2 attached to sensors compared to bulk water communities.

Zone	Site	Sample type	DNA (ng/ μ L)	Richness (OTUs)	Shannon	Simpson	
1	S10	Biofilm	Polyvinyl chloride	6.46	243	2.954	6.962
			Stainless steel	4.06	284	2.973	6.564
			Polyoxymethylene	12.44	267	3.051	10.743
		Water		3.21	360	3.508	0.893
	S11	Biofilm	Polyvinyl chloride	9.53	408	2.599	3.367
			Stainless steel	6.47	188	1.897	2.297
		Polyoxymethylene	5.71	264	2.808	5.625	
		Water		3.63	281	4.030	0.962
2	S14	Biofilm	Stainless steel	3.59	244	3.275	9.955
			Water		5.81	173	2.366
	S15	Biofilm	Stainless steel	11.2	209	3.362	10.682
			Water		3.36	132	2.256

3

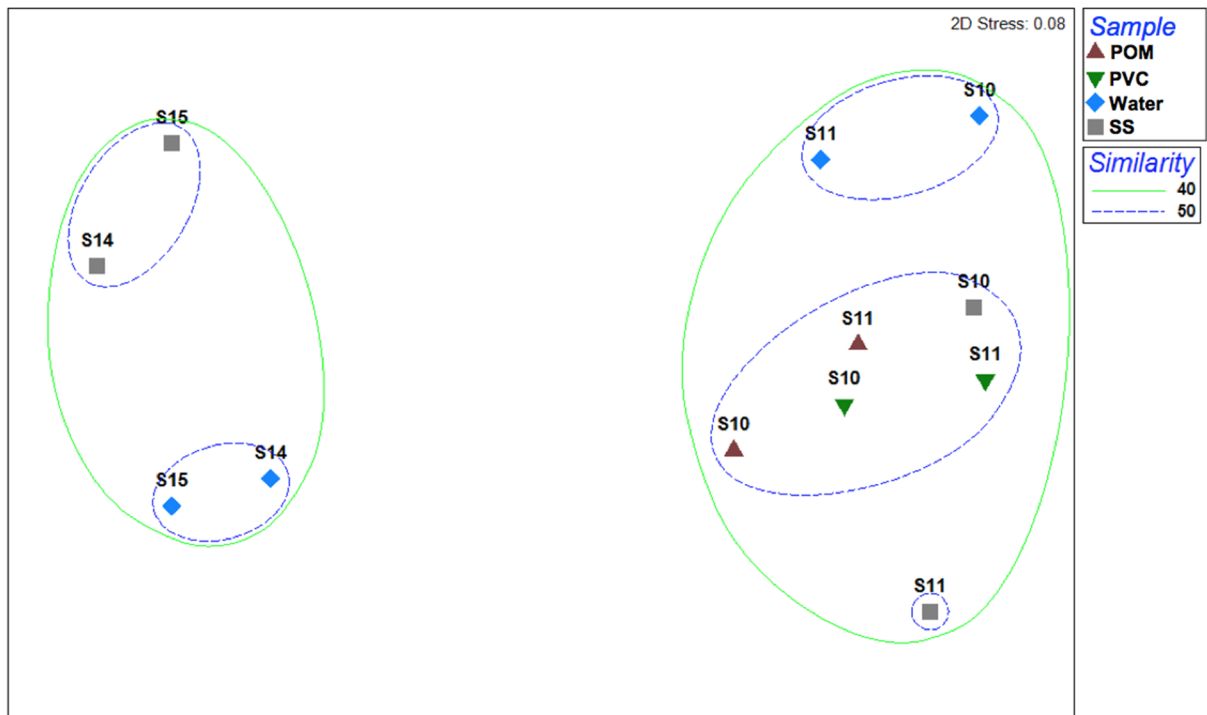


1

2 **Figure 1.** Comparison of microbial composition in biofilms on different types of surfaces (stainless steel [“SS”], polyvinyl chloride [“PVC”],
 3 and polyoxymethylene [“POM”]) and in bulk water collected from four sites. Biofilm and bulk water samples were analyzed without technical
 4 replicates. Results are expressed as relative abundance in total sequencing reads (%) of prokaryotic 16S rRNA genes (including *Archaea* and
 5 *Bacteria*).

6

7



1
 2 **Figure 2.** Non-metric multidimensional scaling (nMDS) analysis of microbial community
 3 composition (including *Archaea* and *Bacteria*) showing clear dissimilarity in community
 4 structure between Zone 1 (S10 and S11) and Zone 2 (S14 and S15) samples. The microbial
 5 community structure was profiled using the sequencing data of 16S rRNA gene amplicons at
 6 the OTU level for biofilm and water samples collected from four sites. Biofilm and bulk
 7 water samples were analyzed without technical replicates. POM, polyoxymethylene; PVC,
 8 polyvinyl chloride; SS, stainless steel.